Commun. Comput. Phys.
doi: 10.4208/cicp.010809.081209a

Vol. **8**, No. 5, pp. 1052-1073
November 2010

Gas Flow Through Square Arrays of Circular Cylinders with Klinkenberg Effect: A Lattice Boltzmann Study

Zhenhua Chai[1,*], Baochang Shi[1], Zhaoli Guo[2] and Jianhua Lu[2]

[1] *School of Mathematics and Statistics, Huazhong University of Science and Technology, Wuhan, 430074, China.*
[2] *State Key Laboratory of Coal Combustion, Huazhong University of Science and Technology, Wuhan, 430074, China.*

Received 1 August 2009; Accepted (in revised version) 8 December 2009

Communicated by Sauro Succi

Available online 31 May 2010

Abstract. It is well known that, as non-continuum gas flows through microscale porous media, the gas permeability derived from Darcy law is larger than the absolute permeability, which is caused by the so-called Klinkenberg effect or slippage effect. In this paper, an effective definition of Knudsen number for gas flows through square arrays of circular cylinders and a local boundary condition for non-continuum gas flows are first proposed, and then the multi-relaxation-time lattice Boltzmann equation including discrete effects on boundary condition is used to investigate Klinkenberg effect on gas flow through circular cylinders in square arrays. Numerical results show that the celebrated Klinkenberg equation is only correct for low Knudsen number, and second-order correction to Klinkenberg equation is necessary with the increase of Knudsen number. Finally, the present numerical results are also compared to some available results, and in general an agreement between them is observed.

PACS: 44.05.+e, 47.11.-j, 47.56.+r

Key words: Klinkenberg effect, multi-relaxation-time lattice Boltzmann equation, Knudsen number, Klinkenberg equation.

1 Introduction

Gas flow in porous media has received an increasing attention for its importance and wide applications in science and engineering [1]. The study on physics of gas flow

*Corresponding author. *Email addresses:* `hustczh@126.com` (Z. Chai), `sbchust@126.com` (B. Shi), `zlguo@hust.edu.cn` (Z. Guo), `lujhhust@gmail.com` (J. Lu)

 ©2010 Global-Science Press

through porous media is necessary to understand deeply some abnormal transport phenomena (e.g., Klinkenberg effect or slippage effect) appeared in petroleum and natural gas industries. Gas slippage phenomena is usually observed in the experiments when gas flow through porous media under low pressure, at which condition the mean free path of the gas molecules is comparable with pore throat radius. Physically speaking, this slippage effect yields a larger effective gas permeability compared to that at high pressure. In the year 1941, Klinkenberg first proposed a formula on the effective gas permeability (K) as [2]

$$K=K_\infty\Big(1+\frac{b_K}{P}\Big), \tag{1.1}$$

which is also called Klinkenberg equation, K_∞ is the absolute or true permeability derived under very large pressure, $b_K=4C_0P\lambda/r$ is the Klinkenberg factor, λ is mean free path of gas molecules, r is the effective pore radius, C_0 is a constant and P is pore pressure. By introducing the Knudsen number (Kn) which is defined as the ratio of molecular mean free path to effective pore diameter ($D_h=2r$), the Klinkenberg equation can be rewritten as

$$K=K_\infty(1+8C_0\times Kn). \tag{1.2}$$

Since the famous experiment conducted by Klinkenberg, many experimental and theoretical studies were carried out to study Klinkenberg effect, and the main focus is to present an explicit expression on Klinkenberg factor b_K [3–12], here some expressions on b_K derived by different authors are summarized in Table 1. With the help of original Klinkenberg equation or these modified equations, some macroscopic properties of flow in porous media can be derived with extended Darcy law. Due to the complexity of porous structure, however, these macroscopic expressions (e.g., extended Darcy law) have no capacity to present detailed resolutions for flow through porous media. As an efficient mesoscopic approach, the lattice Boltzmann equation (LBE) has been a new potential tool and gained much success in simulating flow through porous media at pore scale level for its distinct implementation on boundary conditions [14–21]. On the other hand, due to the kinetic background of LBE, it is also applied to study microscale gaseous flow with non-continuum effect in recent years [22–31]. Above two distinguished characteristics of LBE may make it be very suitable to investigate non-continuum gas flow in porous media.

In the past years, although many works have shown that LBE is capable of simulating flow in porous media, most of the available LBE models are constructed under the continuum assumption, and much less attention has been paid to non-continuum gas flow in porous media. To the authors' knowledge, there is only little work on applying LBE to study non-continuum gas flow in porous media [19–21]. In these published works [19–21], two basic problems have not been solved. One is how to define an effective Knudsen number for gas flow in porous media, and another is how to propose a local boundary condition for non-continuum gas flow and include its discrete effects in LBE [29–31]. Therefore, the objectives of present work are twofold. The first is to

Table 1: The expressions on Klinkenberg factor b_K, [σ is tangential momentum accommodation coefficient].

Literature	b_K	unit
Heid 1950 [3]	$b_k=0.11K_\infty^{-0.39}$	Pa
Jones 1972 [4]	$b_k=6.9K_\infty^{-0.36}$	psi
Jones and Owen 1979 [5]	$b_k=0.86K_\infty^{-0.33}$	Pa
Sampath and Keighin 1982 [6]	$b_k=0.0955(K_\infty/\epsilon)^{-0.53}$	MPa
Jones 1987 [7]	$b_k=16.4K_\infty^{-0.382}$	psi
Woudberg and Du Plessis 2008 [11]	$b_k=12\frac{2-\sigma}{\sigma}Kn\times P\times K_\infty$	—
Tanikaw and Shimamoto 2009 [12]	$b_k=(0.15\pm0.06)K_\infty^{-0.37\pm0.038}$	Pa

present an effective definition on Knudsen number based on theory of hydraulic diameter. The second is to propose a combination of bounce-back and full diffusive boundary condition, and present a strategy to adjust the parameters in this combination boundary conditions such that an accurate slip boundary condition can be implemented. The remainder of the paper is organized as follows. In following Section 2, we extend multi-relaxation-time LBE (MRT-LBE) to study non-continuum gas flow in porous media, and present a detailed discussion on discrete effects on combination of bounce-back and full diffusive (CBBFD) boundary condition. In Section 3, an effective definition on Knundsen number is first proposed, subsequently, the numerical results and related discussions on non-continuum gas flows through square arrays of circular cylinders are presented. Finally, a brief summary of the present work is given in Section 4.

2 Numerical method and boundary condition

As a new numerical method for fluid flows, LBE is first viewed as a successor of lattice gas automata, but it can also be served as a special discrete form of the continuous Boltzmann equation. The most popular LBE used in simulating porous flows is the lattice Bhatnagar-Gross-Krook (BGK) model [32] (see [16, 17, 19–21]). As pointed out in previous works [18, 33], however, a viscosity-dependent permeability is usually derived when lattice BGK model is used in numerical simulations [16, 18]. In fact, the viscosity effect on permeability is induced by numerical slip velocity on solid surface, we refer the reader to [38] for details. In order to overcome the defect inherent in lattice BGK model, the multi-relaxation-time (MRT) model [34–36] and two-relaxation-time (TRT) model [37] has been proposed recently to simulate flows through porous media [18, 33], but to our knowledge, the MRT-LBE has not been extended to simulate non-continuum gas flows in porous media. In following parts, we will limit our attention to MRT-LBE and boundary condition for non-continuum gas flow in porous media.

2.1 Multi-relaxation-time lattice Boltzmann method

For simplicity but without losing generality, here we only consider a two-dimensional MRT-LBE with nine velocities (D2Q9 model). The evolution of LBE with multi-relaxation-

time model can be written as [35,36]

$$f_i(\mathbf{x}+\mathbf{c}_i\delta x,t+\delta t)-f_i(\mathbf{x},t)=\Omega_i+\delta t F_i^{'}, \tag{2.1}$$

where

$$\Omega_i=-\sum_j(\mathbf{M}^{-1}\mathbf{S}\mathbf{M})_{ij}\left[f_j(\mathbf{x},t)-f_j^{(eq)}(\mathbf{x},t)\right]$$

is collision term, f_i is distribution function associated with molecular with velocity $\mathbf{c}_i$ at position x and time t. In D2Q9 model, the discrete velocity $\mathbf{c}_i$ is defined as

$$\mathbf{c}_i=\begin{cases}(0,0), & i=0,\\ (\cos[(i-1)\pi/2],\sin[(i-1)\pi/2])c, & i=1-4,\\ (\cos[(2i-9)\pi/4],\sin[(2i-9)\pi/4])\sqrt{2}c, & i=5-8,\end{cases}$$

where c=$\delta x/\delta t$ and is set to be 1 in this work, δx and δt are the lattice spacing and time step, respectively. $\mathbf{M}$ is a 9×9 transform matrix,

$$\mathbf{M}=\begin{pmatrix} 1 & 1 & 1 & 1 & 1 & 1 & 1 & 1 & 1\\ -4 & -1 & -1 & -1 & -1 & 2 & 2 & 2 & 2\\ 4 & -2 & -2 & -2 & -2 & 1 & 1 & 1 & 1\\ 0 & 1 & 0 & -1 & 0 & 1 & -1 & -1 & 1\\ 0 & -2 & 0 & 2 & 0 & 1 & -1 & -1 & 1\\ 0 & 0 & 1 & 0 & -1 & 1 & 1 & -1 & -1\\ 0 & 0 & -2 & 0 & 2 & 1 & 1 & -1 & -1\\ 0 & 1 & -1 & 1 & -1 & 0 & 0 & 0 & 0\\ 0 & 0 & 0 & 0 & 0 & 1 & -1 & 1 & -1 \end{pmatrix},$$

which projects the distribution function f_i in velocity space onto the moment space

$$\mathbf{m}=(\rho,e,\varepsilon,j_x,q_x,j_y,q_y,p_{xx},p_{xy})^\top=\mathbf{M}\mathbf{f},$$

where $\mathbf{f}=(f_0,f_1,\cdots,f_8)^\top$, ρ is the density, e is the energy, ε is the square of the energy, j_x and j_y correspond to the x and y components of momentum, respectively; q_x and q_y relate to the x and y components of energy flux, p_{xx} and p_{xy} are the diagonal and off-diagonal component of the viscous stress tensor, respectively. $\mathbf{S}=\mathbf{diag}(\tau_0,\tau_1,\cdots,\tau_8)^{-1}$ is a non-negative diagonal matrix with τ_i being relaxation time for ith moment, additionally, it should be noted that the MRT model will reduce to the BGK model when $\tau_i=\tau$ for $i=0-8$. In order to keep $\mathbf{S}$ be consistent with discrete moment $\mathbf{m}$, we rewrite $\mathbf{S}$ as

$$\mathbf{S}=\mathbf{diag}(\tau_\rho,\tau_e,\tau_\varepsilon,\tau_j,\tau_q,\tau_j,\tau_q,\tau_s,\tau_s)^{-1}. \tag{2.2}$$

The equilibrium distribution function $f_i^{(eq)}(x,t)$ in evolution equation (2.1) is usually a function of density ρ and velocity $\mathbf{u}$ and can be given as

$$f_i^{(eq)}=w_i\rho\left[1+3(\mathbf{c}_i\cdot\mathbf{u})+\frac{9}{2}(\mathbf{c}_i\cdot\mathbf{u})^2-\frac{3}{2}\mathbf{u}^2\right], \tag{2.3}$$

where $w_0=4/9$, $w_{1-4}=1/9$, $w_{5-8}=1/36$; F_i' is the discrete forcing term accounting for a body force $\mathbf{F}$, and defined as [29]

$$\mathbf{F}'=\mathbf{M}^{-1}\Big(\mathbf{I}-\frac{\mathbf{S}}{2}\Big)\mathbf{M}\tilde{\mathbf{F}},$$

where $\mathbf{I}$ is unit matrix, $\mathbf{F}'=(F_0',F_1',\cdots,F_8')^\top$, and $\tilde{\mathbf{F}}=(\tilde{F}_0,\tilde{F}_1,\cdots,\tilde{F}_8)^\top$ with

$$\tilde{F}_i=w_i\Big[3\mathbf{c}_i\cdot\mathbf{F}+9\mathbf{u}\mathbf{F}:\Big(\mathbf{c}_i\mathbf{c}_i-\frac{1}{3}\mathbf{I}\Big)\Big].$$

Through the Chapman-Enskog expansion, the Navier-Stokes equation can be derived from present MRT-LBE with an equation of state $P=\rho/3$, the kinematic viscosity is related to the relaxation time τ_s [29,36]

$$\nu=\frac{\delta t}{3}\Big(\tau_s-\frac{1}{2}\Big), \tag{2.4}$$

and the macroscopic density and velocity in MRT-LBE are defined as

$$\rho=\sum_i f_i,\quad \rho\mathbf{u}=\sum_i \mathbf{c}_i f_i+\frac{\delta t}{2}\mathbf{F}.$$

As we know, above MRT-LBE is usually applied to study continuum flows. However, when it is used to study non-continuum gas flows, there are two important issues to be solved properly, the first is how to establish the relationship between the Knudsen number and relaxation time(s), and the second is how to propose a proper boundary condition and include its discrete effects in LBE. For the first issue, Guo et al. have proposed a more reasonable relationship between Kn and relaxation time τ_s as [28]

$$\tau_s=\frac{KnH}{c^*\delta t}+\frac{1}{2}, \tag{2.5}$$

where $c^*=\sqrt{\pi RT/2}$ is a certain microscopic velocity. In this paper, we will adopt this relationship, for another issue, we will discuss it in the following subsection.

2.2 A combination of bounce-back and full diffusive boundary condition for non-continuum gas flow

The kinetic boundary conditions for LBE in simulating non-continuum gas flow is also another important issue, and has been discussed extensively by many authors [22,23,26]. A brief survey on this topic is given in [30]. Although several boundary conditions are existing for non-continuum flow, the discrete effects on these boundary conditions are seldom considered. Ginzbourg and Adler may be the first who give a detailed analysis on discrete effects on boundary conditions for continuum flows [39]. Subsequently, He et al. analyzed several different no-slip boundary conditions in detail, and obtained corresponding analytical solutions of LBE for simple Poiseuille and Couette flows [38].

Recently, Guo et al. [28] studied the discrete effects on the discrete Maxwellian boundary condition and a combination of the bounce-back and specular reflection boundary condition for microscale gas flows, and proposed a strategy to adjust the parameters in the two kinetic boundary conditions such that an accurate slip boundary condition on solid surface can be implemented. However, neither the discrete Maxwellian boundary condition nor the combination of the bounce-back and specular reflection boundary condition can be easily implemented for non-continuum gas flow in porous media since it is hard to ascertain specular reflection directions. Therefore, another CBBFD boundary condition proposed in [30, 31] is used in this work. We would like to point out that the CBBFD scheme is a local boundary condition and possesses more potential in simulating non-continuum flow in a complex geometry. In the following part, the discrete effects on the CBBFD boundary condition will be discussed in detail.

To obtain an analytical solution of MRT-LBE coupling with the CBBFD boundary condition, a unidirectional gas flow over a flat plate is considered (see Fig. 1), and following conditions are assumed to be satisfied

$$\rho = const, \quad v = 0, \quad \frac{\partial \vartheta}{\partial x} = 0,$$

where ϑ is any flow variable. After collision at time t, the unknown distribution functions, f_2^1, f_5^1, and f_6^1, can be determined from the CBBFD boundary condition as

$$\begin{aligned} f_2^1 &= rKf_2^{(eq)}(\mathbf{u}_w) + (1-r)\bar{f}_4^1, \\ f_5^1 &= rKf_5^{(eq)}(\mathbf{u}_w) + (1-r)\bar{f}_7^1, \\ f_6^1 &= rKf_6^{(eq)}(\mathbf{u}_w) + (1-r)\bar{f}_8^1, \end{aligned}$$

where r is a combination parameter, $\mathbf{u}_w$ is the wall velocity, $\bar{f}_i$ is the post-collision distribution function, and defined as

$$\bar{f}_i = f_i - \sum_j (\mathbf{M}^{-1}\mathbf{S}\mathbf{M})_{ij}[f_j - f_j^{(eq)}] + \delta t F_i',$$

$\mathbf{a} = (a, 0)$ (see Fig. 1) is the acceleration corresponding to the body force $\mathbf{F}$. The parameter K is defined as $K = (\bar{f}_4^1 + \bar{f}_7^1 + \bar{f}_8^1)/[f_2^{(eq)} + f_5^{(eq)} + f_6^{(eq)}]$, and can be shown to be 1 for this special case.

Following the approach proposed in some available literature [29–31, 38], we can derive the following equation

$$u_2 = A_1 u_1 + A_2 \delta t a, \tag{2.6}$$

where u_1 and u_2 are velocities at $j=1$ and $j=2$, the parameters A_1 and A_2 are given as

$$\begin{aligned} A_1 &= \frac{3-2r+r\tau_s}{1-r+r\tau_s}, \\ A_2 &= \frac{(\frac{11}{2} - 2\tau_q - 8\tau_s + 4\tau_q\tau_s)r + 4\tau_q + 4\tau_s - 8\tau_q\tau s - 5}{(2\tau_s - 1)(1-r+r\tau_s)}. \end{aligned}$$

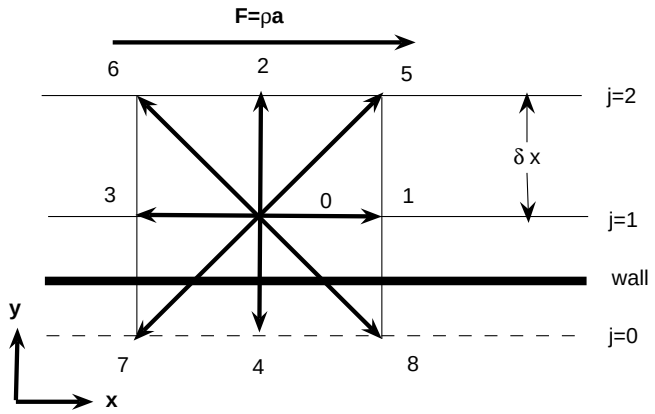

Figure 1: The configuration of lattice in D2Q9 model. The wall (bold line) is placed at j=1/2.

For velocity at inner node ($j\geq 2$), we have

$$\nu\frac{u_{j+1}-2u_j+u_{j-1}}{\delta x^2}+a=0, \tag{2.7}$$

which is just a second-order finite difference equation of the following partial differential equation

$$\nu\frac{\partial^2 u}{\partial x^2}+a=0. \tag{2.8}$$

However, to derive solution of finite difference equation (2.7), we need another boundary condition for velocity. Here, a simple Poiseuille flow is considered, and two walls are fixed at $y=0$ and $y=H$. For such flow, we have following analytical solution [29,38]

$$u_j=4U_0\frac{y_j}{H}\Big(1-\frac{y_j}{H}\Big)+u_s, \tag{2.9}$$

where $y_j=(j-1/2)\delta x$, $U_0=aH^2/8\nu$ is the centerline velocity without slip at solid wall, u_s is slip velocity depending on implementation of boundary condition on solid wall. For CBBFD boundary condition, we can obtain an analytical expression on u_s by substituting Eq. (2.9) into Eq. (2.6)

$$u_s=\frac{2r(2\tau_s-1)}{2-r}U_0\Delta+\frac{[16(\tau_q-\frac{1}{2})(\tau_s-\frac{1}{2})-3]}{3}U_0\Delta^2, \tag{2.10}$$

where $\Delta=\delta x/H$. By introducing a dimensionless slip velocity U_s, we can rewrite Eq. (2.10) as

$$U_s=\frac{u_s}{U_0}=\frac{4r}{2-r}\Big(\tau_s-\frac{1}{2}\Big)\Delta+\frac{[16(\tau_q-\frac{1}{2})(\tau_s-\frac{1}{2})-3]}{3}\Delta^2, \tag{2.11}$$

with the aid of the relationship between τ_s and Kn, i.e., Eqs. (2.5) and (2.11) can be rewritten as

$$U_s = \frac{4r}{2-r}\sqrt{\frac{6}{\pi}}Kn + \frac{2}{\pi}\frac{16(\tau_q-\frac{1}{2})(\tau_s-\frac{1}{2})-3}{(\tau_s-\frac{1}{2})^2}Kn^2. \tag{2.12}$$

Now, we would like to give some remarks on Eq. (2.11) or Eq. (2.12).

Remark 2.1. For purely bounce-back boundary condition (i.e., $r=0$), the slip velocity $U_s \sim \Delta^2$ or $U_s \sim Kn^2$, which is just the fact that half-way bounce-back is a second-order boundary condition [38]. Generally speaking, the numerical slip velocity U_s induced by half-way bounce-back boundary condition can be eliminated as the grid number $N \to \infty$, but it is impossible in practice, especially for simulating flow in porous media. In fact, when LBE is used to simulate flow in porous media, the grid number in one pore is usually very small, and the effect of numerical slip velocity will be significant, which may further influence the permeability computed from the Darcy law. On the other hand, when the grid number in numerical simulation is fixed, the slip velocity is also related to relaxation time(s) or equivalently related to kinematic viscosity ν [see Eq. (2.11)], so it is not surprising that the computed permeability with LBE coupling with BGK model is usually related to kinematic viscosity [16, 18]. However, the numerical slip velocity in MRT-LBE can be eliminated completely by tuning relaxation time τ_q. In fact, the choice of $\tau_q = (8\tau_s-1)/8(2\tau_s-1)$ will lead to $U_s=0$, this result was also reported in some previous studies [33, 39]. To see the viscosity effect on permeability clearly, here we take circular cylinders in square arrays (see Fig. 4, $D_p=0.9025$) as an example, and preset a detailed comparison between BGK model and MRT model with different viscosities in Fig. 2. As shown in this figure, the dimensionless permeability derived with BGK model shows an increase in viscosity, while MRT model gives almost a fixed value, which is in

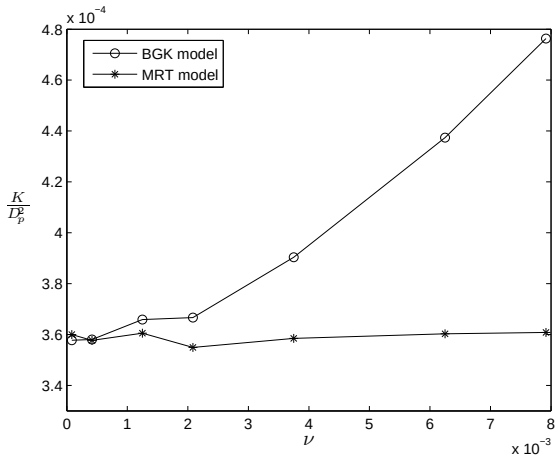

Figure 2: The computed dimensionless permeabilities (K/D_p^2) with BGK model and MRT model are presented under different viscosities (ν) [$\nu=(\tau-1/2)\delta t/3$, where $\tau=0.6,1.0,2.0,3.0,5.0,8.0,10.0$].

good agreement with theoretical value (3.65×10^{-4}) reported by Sangani and Acrivos [44]. Additionally, Fig. 2 also provides an evidence to support MRT model can be used to overcome some nonphysical effects inherent in BGK model.

Remark 2.2. As discussed in Remark 2.1, the numerical slip velocity is not only related to grid number N, but also related to relaxation time(s). When LBE is used to simulate non-continuum gas flow, the relaxation time τ_s is usually larger than that for continuum flow, which leads the numerical slip velocity on solid wall to be more pronounced, so it is necessary to give a strategy that can be used to guarantee an accurate slip boundary condition is implemented.

To match present combination of bounce-back and full diffusive boundary condition for non-continuum gas flow with a more accurate second-order slip boundary condition proposed by Hadjiconstantinou [40], i.e., $U_s=4C_1Kn+8C_2Kn^2$ ($C_1=1.11$ and $C_2=0.61$ are two parameters relating to the gas-wall interaction), the combination parameter r and relaxation time τ_q should be chosen as

$$r=\frac{2C_1}{\sqrt{\frac{6}{\pi}}+C_1},\quad \tau_q=\frac{1}{2}+\frac{3+\pi(2\tau_s-1)^2C_2}{8(2\tau_s-1)}. \tag{2.13}$$

Now, we would like to compare present correction equation (2.13) for MRT-LBE with that for LBE coupling with BGK model [30]. As shown in [30], the combination parameter r for BGK model is given as

$$r=2\left(1+\frac{4\sqrt{\frac{6}{\pi}}Kn}{4C_1Kn+8C_2Kn^2-\frac{32}{\pi}Kn^2+\Delta^2}\right)^{-1}. \tag{2.14}$$

As seen from Eq. (2.14), it is clear that the parameter r, unlike that in MRT-LBE, is not only dependent on gas-solid interaction parameters C_1 and C_2, but also dependent on Kn and grid number through Δ. In what follows, we will carry our some numerical experiments to validate present theoretical results.

Here we choose the Poiseuille flow as a tested example. Periodic boundary conditions are applied to the inlet and outlet of the channel and grid number in x direction is fixed to be 16, the Knudsen number and acceleration are set to be 0.1 and 10^{-4}, respectively. As shown in Fig. 3(a), the discrete effects are clearly observed when the combination r and relaxation time τ_q are chosen arbitrarily. However, when the expressions of r and τ_q given by Eq. (2.13) are used in numerical simulations, it is found that the numerical results are in good agreement with the analytical solution that is derived by solving Navier-Stokes equations coupling with the second-order slip boundary condition proposed by Hadjiconstantinou [40] [see Fig. 3(b)]. Finally, we would like to point out that Verhaeghe et al. have present some similar results, but the first-order slip boundary condition is adopted in their work [31].

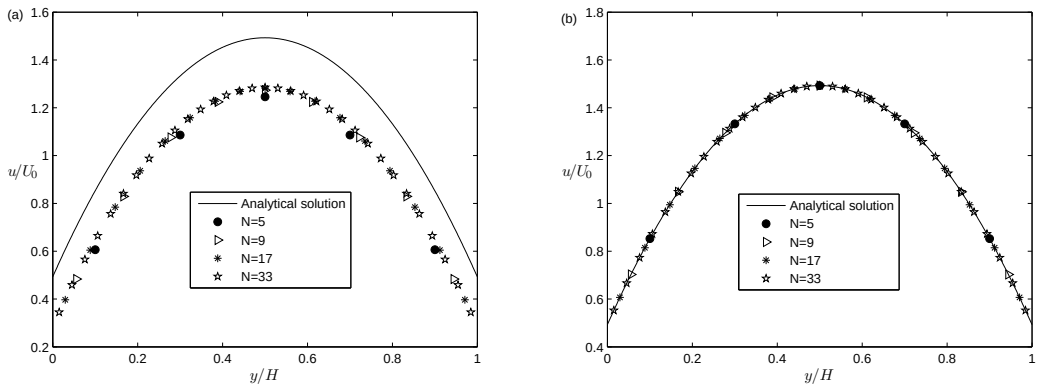

Figure 3: Velocity profile with combination of bounce-back and full diffusive boundary condition. (a) $r=0.5$, $\tau_q=\tau_s$; (b) r and τ_q are given by Eq. (2.13).

3 Numerical results and discussions

The schematic considered in this paper is a two-dimensional region filled with square arrays of circular cylinders (see Fig. 4), which can be viewed as a simple porous media. The width H and length L of the region are set to be 1 and 4, D_p is diameter of circular cylinder, its variance can be used to change porosity (ϵ) of porous media. It should be noted that present two-dimensional schematic can be served as a simplified three-dimensional version in which flow perpendicular to circular cylinders. In the following numerical simulations, periodic boundary conditions are adopted on the top and bottom boundaries, and pressure boundary conditions are used in the horizontal direction. It should be noted that the difference of pressures $\Delta P=P_{in}-P_{out}$ should be small enough, and set to be 3.33×10^{-4} in this study, where P_{in} and P_{out} are pressures at the inlet and outlet, respectively. There are two reasons for the use of small pressure difference, one is to ensure Mach number to be small, and another is to eliminate inertial effect. Unless otherwise mentioned, the non-equilibrium extrapolation scheme proposed by Guo et al. [41] is used to treat inlet and outlet boundary conditions for its good accuracy.

3.1 Validation of the present MRT-LBE

Before we proceed any further, some details used in the following simulations are specified. A pressure difference is maintained by a fixed density at the inlet and outlet, and the gas permeability is computed from pressure and velocity [1]

$$K=\frac{2\mu L\bar{U}_o P_o}{P_i^2-P_o^2}, \tag{3.1}$$

where $\mu=\rho\nu$ is dynamic viscosity, $\bar{U}_o$ is width-averaged seepage velocity at outlet. The Knudsen number in the present work is defined as the ratio between the mean free path

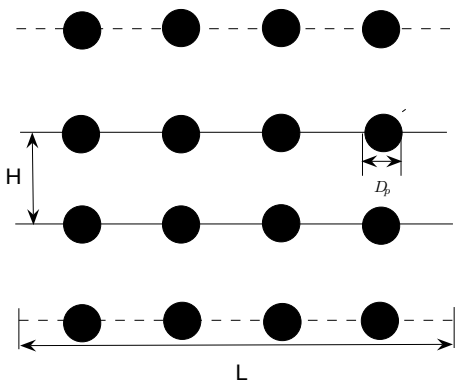

Figure 4: The configuration of circular cylinders in square arrays.

of the gas molecules and mean pore diameter D_{pore}, which is related to the porosity (ϵ) and the specific surface of porous media by using hydraulic diameter concept developed for flow in non-circular conduits. For flow perpendicular to circular cylinders in square arrays, D_{pore} is given as

$$D_{pore}=\frac{\epsilon}{1-\epsilon}D_p, \tag{3.2}$$

and the corresponding definition of the Knudsen number is

$$Kn=\frac{\lambda}{D_{pore}}. \tag{3.3}$$

Compared with available definitions on Kn [19–21], Eq. (3.3) may be more reasonable by including the effects of diameter of circular cylinder and porosity of porous media. In addition, we also note that the hydraulic diameter concept was also used by de Socio and Marino to study gas flow through porous media filled with compacted glass spheres [9].

Table 2: Grid number ($M\times N$) effect on permeability (K) of circular cylinders in square arrays with $D_p=0.8025$ [M, N are the grid numbers corresponding to the width H and length L].

Grid number ($M\times N$)	51×201	101×401	201×401	401×801	801×3201
Permeability (K)	1.652×10^{-3}	1.701×10^{-3}	1.740×10^{-3}	1.766×10^{-3}	1.761×10^{-3}

We first present the grid number effect on the permeability of circular cylinders with $D_p=0.8025$ in continuum regime ($Kn=10^{-4}$), and show the results in Table 2. As seen from this table, the grid number fixed at 401×801 is large enough to derive grid-independent results, and this grid number will be adopted in the following simulations.

To valid present MRT-LBE, we compare the computed permeability of circular cylinders in square arrays at $Kn=10^{-4}$ (see Table 3 for details) with some available results in Fig. 5. As shown in this figure, the present numerical results are in good agreement with these available experimental, theoretical and numerical results [42–44].

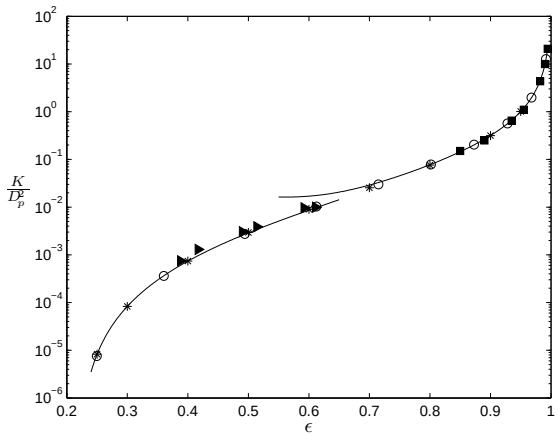

Figure 5: The dimensionless permeability for different porosity. ○, present numerical results ($Kn=10^{-4}$); ■, experimental results (Kirsch and Fuchs, 1967); ▶, experimental results (Sadiq, Advani and Parnas, 1995); $*$, numerical results (Sangani and Acrivos, 1982); $-$, theoretical results (Sangani and Acrivos, 1982).

In the following parts, we will investigate the effects of Knudsen number on gas permeability and fluid flow field, but only near continuum gas flow ($Kn \leq 0.25$) in porous media is considered.

3.2 Theoretical and numerical results on gas permeability

Physically speaking, the increase of Knudsen number will reduce the interaction between gas molecules and the solid walls. As a result, a slip velocity on solid surface is induced, which leads the gas permeability to be larger than that at the continuum level. From a theoretical point of view, we can derive the gas permeability of some ideal porous media.

3.2.1 Gas permeability of a porous media composed of a bundle of channels or tubes

Considering a porous medium composed of a bundle of parallel and straight channels and gas flow in near-continuum regime, we can use the Navier-Stokes equations coupling with the second-order slip boundary condition [40] to derive the gas permeability, which can be written as [20]

$$K=K_\infty(1+6C_1Kn+12C_2Kn^2), \tag{3.4}$$

where $K_\infty = Nh^3/12$ is absolute permeability, h is height of channel, N is the number of channel per cross-sectional area of the porous media. Similar to above discussion, for ideal porous media composed of circular tubes with equal diameter D, the corresponding gas permeability is derived as

$$K=K_\infty(1+8C_1Kn+16C_2Kn^2), \tag{3.5}$$

with $K_\infty = N\pi D^4/128$. Additionally, the different values of C_1 and C_2 proposed by other authors can be found in [20].

3.2.2 Gas permeability of a porous media composed of circular cylinders in square arrays

For Newtonian fluid flow through the cell geometry (see Fig. 4) with second-order slip boundary proposed by Hadjiconstantinou [40], the relationship between pressure drop and flow rate (Q) can be derived with lubrication theory that is only valid for low porosity

$$\frac{\partial P}{\partial x}=\frac{12\mu Q}{H_R^3+6C_1\lambda H_R^2+12C_2\lambda^2 H_R}, \tag{3.6}$$

where $H_R=H-2\sqrt{R^2-x^2}$, $R=D_p/2$ is radius of circular cylinder. We can further integrate Eq. (3.6) over the length of the unit cell, and derive pressure drop over the cylinder

$$\Delta P_R=\int_0^R \frac{12\mu Q}{H_R^3+6C_1\lambda H_R^2+12C_2\lambda^2 H_R}dx. \tag{3.7}$$

With the help of Darcy law

$$\bar{U}=Q/H=-\frac{2K}{\mu}\frac{\Delta P_R}{H},$$

we can derive gas permeability as

$$K=\frac{1}{24\displaystyle\int_0^R \frac{1}{H_R^3+6C_1\lambda H_R^2+12C_2\lambda^2 H_R}dx}. \tag{3.8}$$

Although the denominator of Eq. (3.8) can be computed analytically, the final expression of K is very complicated and not presented here. In addition, we would like to point out that, as $\lambda/H_R\to 0$, Eq. (3.8) will reduce to continuum results reported in [45].

As seen from above discussions, the coefficients of first-order and seconder-order of Knudsen number are different from each other even for these ideal porous media, so it is impossible to present two deterministic coefficients for non-continuum gas flow through real porous structures as those for gas flow in microchannels or circular tubes.

We can compute the permeabilities at different porosities and Knudsen numbers with Eq. (3.1), and also plot them in Fig. 6. From this figure, we can find that the gas permeability is a function of both Knudsen number and porosity. When the value of porosity is fixed, the gas permeability increases in Kn and a quadratic relationship between them is observed for all porosity considered in this work, which is consistent with above theoretical Eqs. (3.4) and (3.5). To obtain an explicit formula to express gas permeability, a quadratic curve is used to fit present numerical results, and the coefficients of first-order and seconder-order of Knudsen number, B_1, B_2 and reciprocal (K_r) of the fitting quadratic curve are listed in Table 3. As seen from this table, the coefficients B_1 and B_2 show a similar trend, i.e., they first decrease to a minimum value and then increases with the increase of diameter of circular cylinder, but the value of the coefficient B_2 is larger

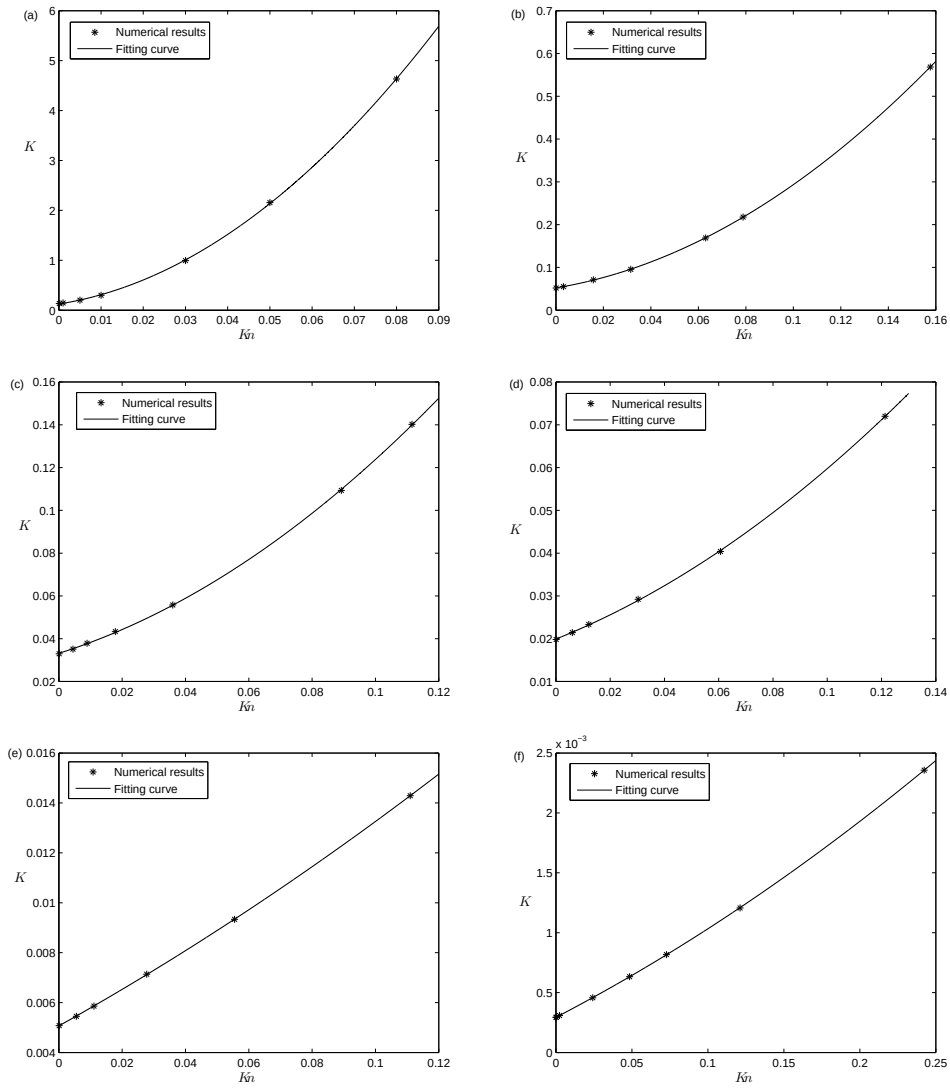

Figure 6: Gas permeability at different porosity and Knudsen number. (a) $D_p=41\delta x$; (b) $D_p=121\delta x$; (c) $D_p=161\delta x$; (d) $D_p=201\delta x$; (e) $D_p=281\delta x$; (f) $D_p=361\delta x$.

than B_1. In addition, we also find that the intercept of the fitting curve or extrapolated absolute permeability K_e is in good agreement with that at $Kn=10^{-4}$.

On the other hand, although the present numerical results generally agree with some previous numerical, theoretical and experimental results [9, 19–21], some differences between them are also observed. For example, Jeong et al. found that the dimensionless permeability is almost a linear function of Kn for gas flow in slip regime ($0.01<Kn<0.1$). There are some reasons accounting for this difference. First of all, different boundary conditions for slip velocity on the solid surface are adopted. In [19], to reflect the slip ve-

Table 3: The coefficients B_1, B_2 and intercept (K_e) of the fitting curve in Fig. 6, [K_∞ is the value at $Kn=10^{-4}$].

D_p	B_1	B_2	K_e	K_∞
$41\delta x$	1.072×10^{2}	4.352×10^{3}	1.239×10^{-1}	1.336×10^{-1}
$81\delta x$	3.668×10^{1}	7.526×10^{2}	7.717×10^{-2}	8.099×10^{-2}
$121\delta x$	1.760×10^{1}	2.869×10^{2}	5.212×10^{-2}	5.194×10^{-2}
$161\delta x$	1.411×10^{1}	1.321×10^{2}	3.317×10^{-2}	3.295×10^{-2}
$201\delta x$	1.274×10^{1}	7.251×10^{1}	1.992×10^{-2}	1.982×10^{-2}
$241\delta x$	1.234×10^{1}	4.591×10^{1}	1.093×10^{-2}	1.088×10^{-2}
$281\delta x$	1.402×10^{1}	2.146×10^{1}	5.065×10^{-3}	5.076×10^{-3}
$321\delta x$	1.582×10^{1}	1.749×10^{1}	1.763×10^{-3}	1.766×10^{-3}
$361\delta x$	2.252×10^{1}	2.687×10^{1}	2.933×10^{-4}	2.936×10^{-4}
$391\delta x$	7.407×10^{1}	3.261×10^{2}	7.093×10^{-6}	7.237×10^{-6}

locity on solid surface, they simply assumed that the particle distribution function after collision at the surface equals equilibrium distribution function. Secondly, the discrete effects on boundary condition is not considered in [19]. As discussed in [29,30,38], when a boundary condition is implemented in LBE, a numerical slip velocity will be induced on solid surface, which may further affect the computed permeability. At last, different definitions on Kn are used in [19] and the present work. The definition on Kn proposed in the present work, i.e., Eq. (3.3), presents a larger value than that in [19] for a larger porosity and vice versa. Tang et al. adopted a combination of the bounce-back and specular reflection boundary condition [23] to describe slip velocity at solid surface and reported similar results to those in this work [20]. To derive the correct slip velocity, however, how to choose the value of bounce-back probability r is also an open problem for this boundary condition. On the other hand, it may be hard to ascertain specular reflection directions for gas flow through more complex porous structures. de Socio and Marino studied gas flow in permeable media both experimentally and numerically, and found that gas permeability is proportional to square of Kn ($K=4.25\times10^{-9}Kn^2$) when Kn is changed from 0.01 to 8 [9]. The main characteristic of this formula is that the zero-order and first-order terms of Kn are not included. Although above formula agrees with their numerical results, it also has limitations from a theoretical point of view. As seen from this formula, the gas permeability K approaches to zero when $Kn\to0$, which violates the fact that gas permeability will reduce to absolute permeability as $Kn\to0$. The reason accounting for de Socio and Marino's formula may be that, the Klinkenberg effect is usually observed in low permeability porous media, the absolute permeability of which is usually very small compared to gas permeability at large Kn.

Compared to the theoretical Eqs. (3.4) and (3.5), the Klinkenberg equation (1.2) only includes first-order term of Knudsen number, so it may be correct for small Kn. To validate this statement, we take the case of $R=180.5\delta x$ as an example and compute gas permeability at small Kn. The numerical results shown in Fig. 7 present a linear relationship between gas permeability K and Kn when Kn is less than 0.01, that is to say, the

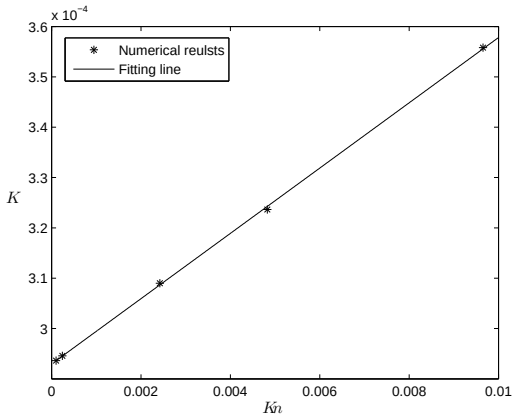

Figure 7: Gas permeability of $D_p = 361\delta x$ at small Knudsen numbers.

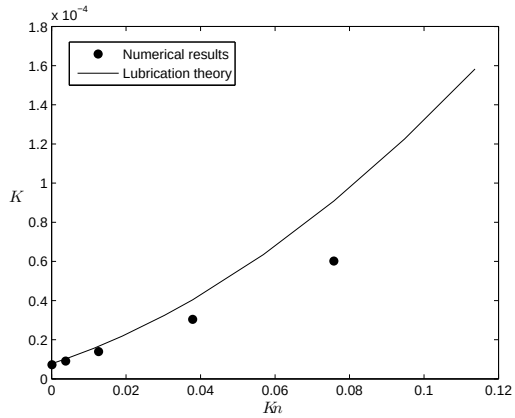

Figure 8: Comparison between present numerical results and lubrication theory at different Knudsen numbers for $D_p = 391\delta x$.

Klinkenberg equation (1.2) is only valid for small Kn. In addition, we also find that the slop of the fitting line is 22.14, which is very close to 22.52 in Table 3.

Finally, we also compare the present numerical results for low porosity with those derived from the lubrication theory. As seen from Fig. 8, although the present numerical results show a similar trend with those derived from lubrication theory, the difference between them is more significant for larger Kn. The reason for this deviation may be that the definition on Kn [i.e., Eq. (3.3)] used in present work is different from the real one used in Eq. (3.8).

3.3 Effect of the Knudsen number on flow field

To see the Klinkenberg effect clearly, the velocity vectors of $R = 60.5\delta x$, $R = 100.5\delta x$, $R = 140.5\delta x$, $R = 180.5\delta x$ at different Kn are plotted in Figs. 9-12. As shown in these figures,

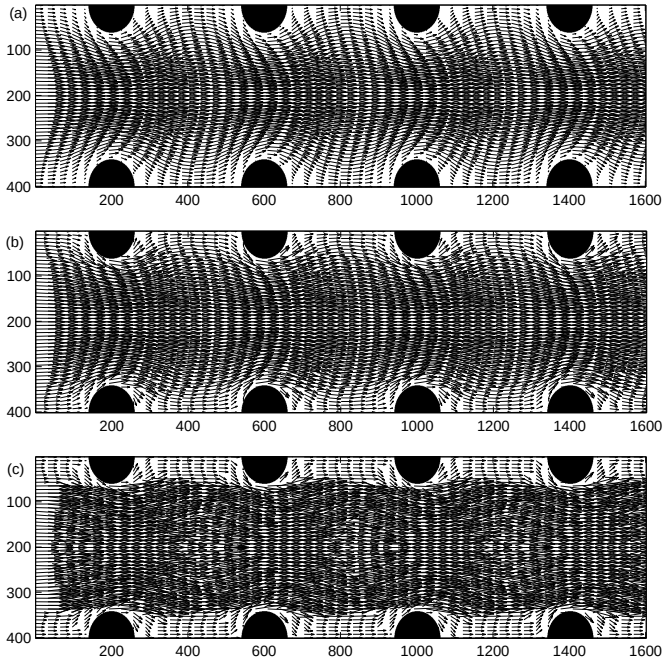

Figure 9: Flow fields at different Knudsen number (D_p=121δx). (a) Kn=10^{-4}; (b) Kn=0.0315; (c) Kn=0.158.

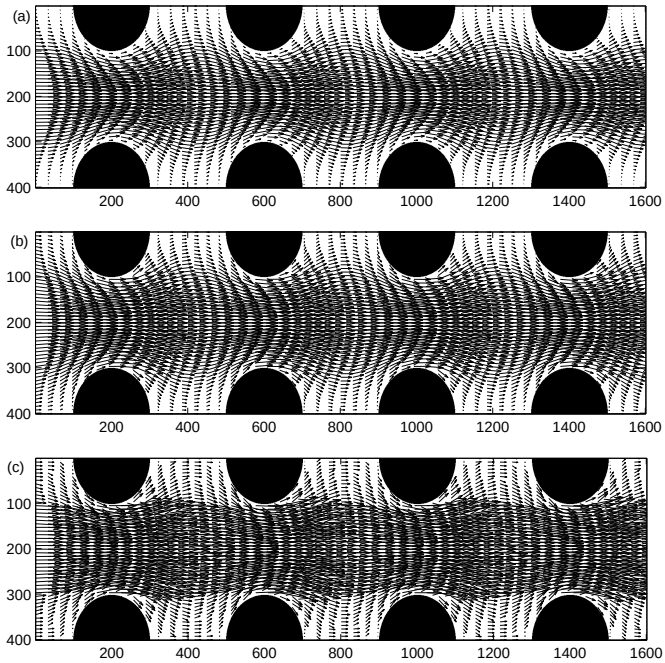

Figure 10: Flow fields at different Knudsen number (D_p=201δx). (a) Kn=10^{-4}; (b) Kn=0.0303; (c) Kn=0.121.

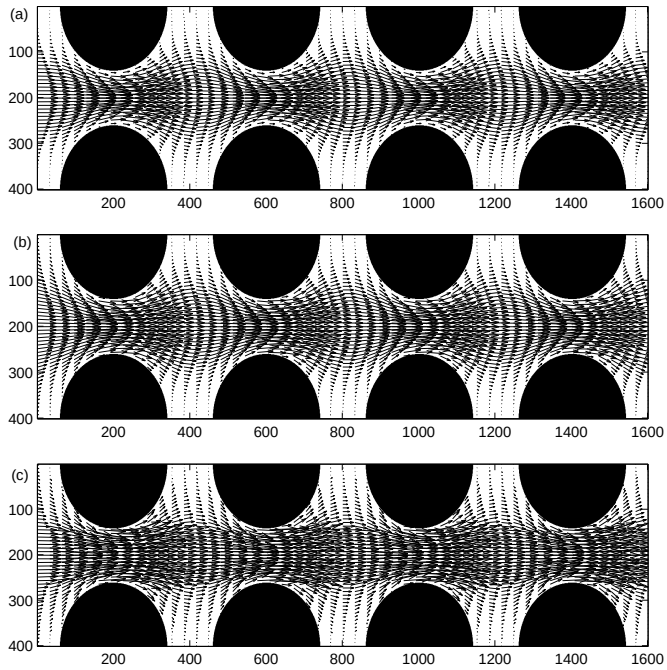

Figure 11: Flow fields at different Knudsen number (D_p=281δx). (a) Kn=10^{-4}; (b) Kn=0.0277; (c) Kn=0.11.

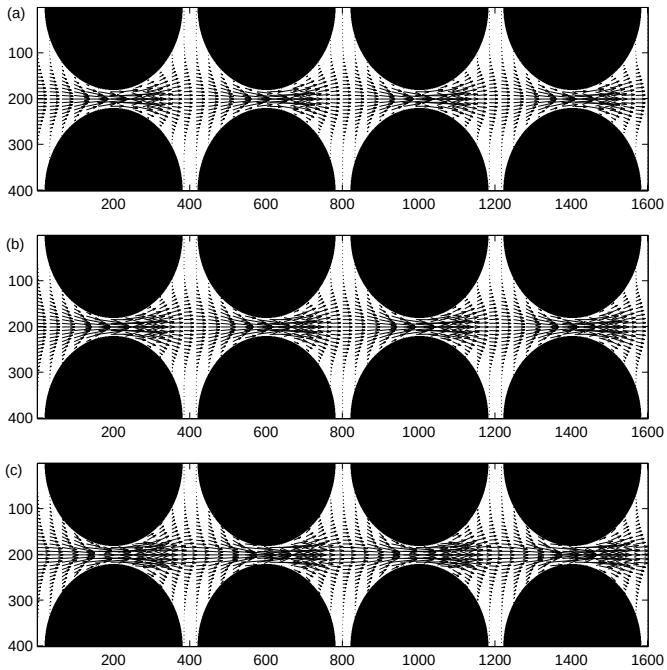

Figure 12: Flow fields at different Knudsen number (D_p=361δx). (a) Kn=10^{-4}; (b) Kn=0.024; (c) Kn=0.12.

some similar results are observed, i.e., the slip velocity on solid wall increases in Kn and the slippage effect or Klinkenberg effect is more pronounced for larger Kn. As described previously, for the cases of $Kn = 10^{-4}$ [see Fig. 9(a)], the slip velocity on solid surface is almost zero, and the velocity vectors are similar to those described by the continuum Stokes equation (the Reynolds number in present work is very small). However, when Kn is increased to some extent [see Fig. 9(b)], the slip phenomena on solid surface is more obvious and the velocity vectors in bulk region are more straight in horizontal direction since the friction drag between gas and solid surface is reduced with the increase of Kn. With further increase of Knudsen number, as shown in Fig. 9(c), the slip velocity on solid surface is much larger and the slippage effect is more pronounced.

4 Summary

In this paper, the multi-relaxation-time lattice Boltzmann equation coupling with the combination of bounce-back and full diffusive boundary condition is proposed to investigate non-continuum gas flow through circular cylinders in square arrays, and present Klinkenberg effects on gas permeability and flow field. Some conclusions are summarized as follows:

(i) A combination of bounce-back and full diffusive boundary condition for non-continuum gas flows is proposed, and the discrete effects on this boundary condition are analyzed in detail.

(ii) Based on lubrication theory, an theoretical expression for non-continuum gas flow through circular cylinders in square arrays is derived.

(iii) The gas permeability is function of Knudsen number and porosity, and a quadratic relationship between gas permeability and Knudsen number is observed for a fixed porosity.

(iv) The Klinkenberg equation is only suitable for low Knudsen number, and second-order correction to Klinkenberg equation is necessary with the increase of Knudsen number.

(v) A larger slip velocity and more pronounced slippage phenomena on solid surface of circular cylinder will be observed for a larger Knudsen number.

It should be noted that the theoretical results on discrete effect of CBBFD boundary condition is derived for gas flow in a smooth channel, but they were used to study gas flow through circular cylinders in square arrays. There are some reasons for above approximate treatment. The first is that it is hard to derive analytical solution of MRT-LBE for gas flow in a complex geometry, so we can not present a further analysis on discrete effect of boundary condition. The second is based on an assumption which may be reasonable in some degree, i.e., the Hagen-Poiseuille law is assumed to be true for flow between two neighboring cylinders. The third is similar treatment for continuous flow through simplified porous media has been reported in available literature (see [18]),

and what is more, these published results unambiguously show that above approximate treatment can be used to improve the accuracy of numerical results.

We also would like to point out that the circular cylinders in square arrays is only an ideal porous structure and may differ much from more realistic porous media, the possible differences between them will be investigated in the future.

Acknowledgments

One of authors (Z. Chai) is grateful to Liang Yu for useful discussions and Professor A. Nakayama at Shizuoka University, Professor I. N. Larina at Russian Academy of Science and Professor T. Staffan Lundström at Luleå University of Technology for sharing some materials. This work is financially supported by the National Basic Research Program of China (Grant No. 2006CB705804) and the National Natural Science Foundation of China (Grant Nos. 60773195 and 10972087).

References

[1] A. E. Scheidegger, The Physics of Flow through Porous Media, University of Toronto, Toronto, 1974.
[2] L. J. Klinkenberg, The perpeability of porous media to liquid and gases, American Petroleum Institute, Drilling and Productions practices, New York, 1941.
[3] J. G. Heid, J. J. Mcmahon, R. F. Nielsen and S. T. Yuster, Study of the permeability of rocks to homogeneous fluids, American Petroleum Institute, Drilling and Productions practices, New York, 1950.
[4] S. C. Jones, A rapid accurate unsteady-state Klinkenberg permeameter, Soc. Pet. Engr. J., 3535(1972), 383-397.
[5] F. O. Jones and W. W. Owen, A laboratory study of low permeability gas sands, J. Pet. Technol., 32(1980), 1631-1640.
[6] K. Sampath and C. W. Keighin, Factors affecting gas slippage in tight sandstones, Soc. Pet. Engr. J., 9872(1982), 409-415.
[7] S. C. Jones, Using the inertial coefficient, β, to characterise heterogeneity in reservoir rock, Paper SPE 16949 presented at 62nd. Annual Technical Conference of Society of Petroleum Engineers, New Orleans, 1987.
[8] Y. S. Wu, K. Pruess and P. Persoff, Gas flow in porous media with Klinkenberg effects, Transp. Porous Med., 32(1998), 117-137.
[9] L. M. de Socio and L. Marino, Gas flow in a permeable medium, J. Fluid Mech., 557(2006), 119-133.
[10] F. A. Florece, J. A. Rushing, K. E. Newsham and T. A. Blasingame, Improved permeability prediction relations for low permability sands, Paper SPE 107954 presented at Rocky Mountain Oil & Gas Technology Symposium of Society of Petroleum Engineers, Colorado, 2007.
[11] S. Woudberg and J.P. Du Plessis, Predicting the permeability of very low porosity sandstones, Transp. Porous Med., 73(2008), 39-55.
[12] W. Tanikawa and T. Shimamoto, Comparison of Klinkenberg-corrected gas permeability and water permeability in sedimentary rocks, Int. J. Rock Mech. Min. Sci., 46(2009), 229-238.

[13] R. N. Xu and P. X. Jiang, Numerical simulation of fluid flow in microporous media, Int. J. Heat Fluid Flow, 29(2008), 1447-1455.
[14] A. Cancelliere, C. Chang, E. Foti, D.H. Rothman and S. Succi, The permeability of a random medium: Comparison of simulation with theory, Phys. Fluids A, 2(1990), 2085-2088.
[15] S. Succi, The Lattice Boltzmann Equation for Fluid Dynamics and Beyond, Oxford University press, Oxford, 2001.
[16] B. Ferréol and D. H. Rothman, Lattice-Boltzmann simulations of flow through fontainebleau sandstone, Transp. Porous Med., 20(1995), 3-20.
[17] A. Koponen, D. Kandhai, E. Hellén, M. Alava, A. Hoekstra, M. Kataja, K. Niskanen, P. Sloot and J. Timonen, Permeability of Three-Dimensional Random Fiber Webs, Phys. Rev. Lett., 80(1998), 716-719.
[18] C. Pan, L.-S. Luo and C. T. Miller, An evaluation of lattice Boltzmann schemes for porous medium flow simulation, Comput. Fluids, 35(2006), 898-909.
[19] N. Jeong, D. H. Choi and C. L. Lin, Prediction of Darcy-Forchheimer drag for micro-porous structures of complex geometry using the lattice Boltzmann method, J. Micromech. Microeng., 16(2006), 2240-2250.
[20] G. H. Tang, W. Q. Tao and Y. L. He, Gas slippage effect on microscale porous flow using the lattice Boltzmann method, Phys. Rev. E, 72(2005), 056301.
[21] G. H. Tang, W. Q. Tao and Y. L. He, Three-dimensional lattice Boltzmann model for gaseous flow in rectangular microducts and microscale porous media, J. Appl. Phys., 97(2005), 104918.
[22] X. Nie, G. D. Doolen and S. Chen, Lattice-Boltzmann simulations of fluid flows in MEMS, J. Stat. Phys., 107(2002), 279-289.
[23] S. Succi, Mesoscopic modeling of slip motion at fluid-solid interfaces with heterogeneous catalysis, Phys. Rev. Lett., 89(2002), 064502.
[24] M. Sbragaglia and S. Succi, Analytical calculation of slip flow in lattice Boltzmann models with kinetic boundary conditions, Phys. Fluids, 17(2005), 093602.
[25] L. Szalmás, Knudsen layer theory for high-order lattice Boltzmann models, Europhys. Lett., 80(2007), 24003.
[26] S. Ansumali and I. V. Karlin, Kinetic boundary conditions in the lattice Boltzmann method, Phys. Rev. E, 66(2002), 026311.
[27] S. Ansumali, I. V. Karlin, S. Arcidiacono, A. Abbas and N. Prasianakis, Hydrodynamics beyond Navier-Stokes: Exact Solution to the Lattice Boltzmann Hierarchy, Phys. Rev. Lett., 98(2007), 124502.
[28] Z. L. Guo, T. S. Zhao and Y. Shi, Physical symmetry, spatial accuracy, and relaxation time of the lattice Boltzmann equation for microgas flows, J. Appl. Phys., 99(2006), 074903.
[29] Z. L. Guo and C. G. Zheng, Analysis of lattice Boltzmann equation for microscale gas flows: Relaxation time, Boundary condiction, and Knudsen layer, Int. J. Comput. Fluid Dyn., 22(2008), 465-473.
[30] Z. H. Chai, Z. L. Guo, L. Zheng and B. C. Shi, Lattice Boltzmann simulation of surface roughness effect on gaseous flow in a microchannel, J. Appl. Phys., 104(2008), 014902.
[31] F. Verhaeghe, L.-S. Luo and B. Blanpain, Lattice Boltzmann modeling of microchannel flow in slip flow regime, J. Comput. Phys., 228(2009), 147-157.
[32] Y. H. Qian, D. d'Humires and P. Lallemand, Lattice BGK models for Navier-Stokes equation, Europhys. Lett., 17(1992), 478-484.
[33] I. Ginzburg and D. d'Humières, Multireflection boundary conditions for lattice Boltzmann models, Phys. Rev. E, 68(2003), 066614.

[34] F. Higuera, S. Succi and R. Benzi, Lattice gas-dynamics with enhanced collisions, Europhys. Lett. 9(1989), 345-349.
[35] D. d'Humières, in Rarefied Gas Dynamics: Theory and Simulations, Progress in Astronautics and Aeronautics, edited by Shizgal B D and PWeaver D, AIAA Press,Washington, DC, 159(1992), 450-458.
[36] P. Lallemand and L.-S. Luo, Theory of the lattice Boltzmann method: Dispersion, dissipation, isotropy, Galilean invarioance and stability, Phys. Rev. E, 61(2000), 6546-6562.
[37] I. Ginzburg, F. Verhaeghe and D. d'Humières, Two-relaxation-time lattice Boltzmann scheme: About parametrization, velocity, pressure and mixed boundary conditions, Commun. Comput. Phys., 3 (2008), pp. 427-478.
[38] X. He, Q. Zou, L.-S. Luo and M. Dembo, Analytic solutions of simple flows and analysis of nonslip boundary conditions for the lattice Boltzmann BGK model, J. Stat. Phys., 87(1997), 115-136.
[39] I. Ginzbourg and P. M. Adler, Boundary flow condition analysis for the three-dimensional lattice Boltzmann model, J. Phys. II, 4(1994), 191-214.
[40] N. G. Hadjiconstantinou, Comment on Cercignani's second-order slip coefficient, Phys. Fluids, 15(2003), 2352-2354.
[41] Z. L. Guo, C. G. Zheng and B. C. Shi, Non-equilibrium extrapolation method for velocity and pressure boundary conditions in the lattice Boltzmann method, Chin. Phys., 11(2002), 366-374.
[42] A. A. Kirsch and N. A. Fuchs, Studies on fibrous aerosol filters-II Pressure drops in systems of parallel cylinders, Ann. Occup Hyg., 10(1967), 23-30.
[43] T. A. K. Sadiq, S. G. Advani and R. S. Parnas, Experimental investigation of transverse flow through aligned cylinders, Int. J. Multiphase flow, 21(1995), 755-774.
[44] A. S. Sangani and A. Acrivos, Slow flow past periodic arrays of cylinders with application to heat transfer, Int. J. Multiphase flow, 8(1982), 193-206.
[45] M. V. Bruschke and S. G. Advani, Flow of generalized Newtonian fluids across a periodic array of cylinders, J. Rheol., 37(1993), 479-497.